Ferroelectrics

ISSN: 0015-0193 (Print) 1563-5112 (Online) Journal homepage: http://www.tandfonline.com/loi/gfer20

Optical Properties of the Narrow-Band Ferroelectrics: First Principle Calculations

Husnu Koc, Sevket Simsek, Amirullah M. Mamedov & Ekmel Ozbay

To cite this article: Husnu Koc, Sevket Simsek, Amirullah M. Mamedov & Ekmel Ozbay (2015) Optical Properties of the Narrow-Band Ferroelectrics: First Principle Calculations, Ferroelectrics, 483:1, 43-52, DOI: 10.1080/00150193.2015.1058672

To link to this article: http://dx.doi.org/10.1080/00150193.2015.1058672

Published online: 29 Oct 2015.

Ferroelectrics, 483: 43–52, 2015

ISSN: 0015-0193 print / 1563-5112 online
DOI: 10.1080/00150193.2015.1058672

Optical Properties of the Narrow-Band Ferroelectrics: First Principle Calculations

HUSNU KOC,[1] SEVKET SIMSEK,[2]
AMIRULLAH M. MAMEDOV,[3,4,*] AND EKMEL OZBAY[3]

[1]Department of Physics, Siirt University, 56100 Siirt, Turkey
[2]Department of Material Science and Engineering, Hakkari University, Hakkari Turkey
[3]Nanotechnology Research Center (NANOTAM), Bilkent University, 06800 Bilkent, Ankara, Turkey
[4]International Scientific Center, Baku State University, Baku, Azerbaijan

Based on density functional theory, we have studied the electronic, and optical properties of narrow-band ferroelectric compounds – (Ge,Sn) Te. Generalized gradient approximation has been used for modeling exchange-correlation effects. The lattice parameters of the considered compounds have been calculated. The calculated electronic band structure shows that GeTe and SnTe compounds have a direct forbidden band gap of 0.742 eV and 0.359 eV. The real and imaginary parts of dielectric functions and therefore, the optical functions such as energy-loss function, as well as the effective number of valance electrons and the effective optical dielectric constant are all calculated. Our structural estimation and some other results are in agreement with the available experimental and theoretical data.

Keywords ab initio calculation; electronic structure; optical properties

1. Introduction

A^4B^6 (A = Ge, Sn, Pb; B=Te, Se, S) are the interesting materials from both fundamental and industrial perspectives. When alloyed with Sb, the optical and electronic properties of A^4B^6 become dramatically modified due to the change in the structure from the crystalline to the amorphous phase [1–2]. This makes A^4B^6 the crucial base materials for optical storage rewritable devices. Besides the industrial interest, A^4B^6 compounds also attract fundamental interest for their ferroelectric and electronic properties. At higher temperatures, they possess a highly symmetric, non-polar, and rocksalt cubic structure (Fm3m). Below a critical temperature T_c, they stabilize in a lower symmetry polar structure (R3m) with A- and B-ions being displaced from ideal rocksalt sites. The polar (ferroelectric) transition is characterized by the softening of a zone-center transverse optic phonon mode propagating in the [111] direction and the freezing in of a relative displacement of the crystal sublattices [3]. Due to their interesting properties as ferroelectric and phase change

Received October 2, 2014; in final form April 14, 2015.
*Corresponding author. E-mail: mamedov@bilkent.edu.tr
Color versions of one or more figures in this article can be found online at www.tandfonline.com/gfer.

materials, A^4B^6 compounds have been the subject of many experimental and theoretical studies. The electronic, structural, and optical properties have been investigated in the different phases [1, 3–7].

On the other hand, many emerging phenomena in A^4B^6 compounds are explained by the notion of elementary excitations between them. While the phases are usually topologically referred to as a geometrical characteristic of their electronic structures at equilibrium conditions, it is also of great physical interest to explore whether the elementary excitations or interactions between them can lead to the development of topological phases or to new emerging phenomena associated with the topological phases (PbTe, SnTe, GeTe). It is very viable in these compounds that the interplay of crystalline symmetries and the time-reversal symmetry leads to the very rich behavior of topological phases [8–14].

In this work, we present the first principle calculation of optical and electronic properties of GeTe and SnTe compounds in both the ferroelectric (rhombohedral) and paraelectric (cubic) phases.

2. Method of Calculation

In this study, all of our calculations have been performed using the ab-initio total-energy and molecular-dynamics program VASP (Vienna ab-initio simulation program) developed at the Faculty of Physics of the University of Vienna [15–18] within the density functional theory (DFT) [19]. The exchange-correlation energy function is treated within the GGA (generalized gradient approximation) by the density functional of Perdew et al. [20]. The potentials used for the GGA calculations take into account the $4s^24p^2$ valence electrons of each Ge-, $5s^25p^2$ valence electrons of each Sn-, and $5s^25p^4$ valence electrons of each Te-atoms. The GGA calculation within the core-state model potential of A(Ge, Sn) has only four valence electrons because the $3d^{10}$ and $4d^{10}$ have become part of the core. Pseudopotentials are known for being relatively hard, and the properties investigated in this work are well converged when including a plane-wave basis up to a kinetic-energy cutoff equal to 17 Ha. The Brillouin-zone integration was performed using special k points sampled within the Monkhorst-Pack scheme [21]. We found that a mesh of $12 \times 12 \times 12$ k points was required to describe well of these electronic and optical properties. This k-point mesh guarantees a violation of charge neutrality less than 0.008e. Such a low value is a good indicator for an adequate convergence of the calculations.

3. Results and Discussion

3.1. Structural Properties and Electronic Properties

In the first step of our calculations, we have calculated the equilibrium lattice constants of GeTe and SnTe in both ferroelectric and paraelectric phases. Our obtained results are shown in Table 1 along with the experimental and theoretical results [7, 22–23].

The band structure of GeTe and SnTe along the principal symmetry directions have been calculated by using the equilibrium lattice constants as shown in Table 1 in ferroelectric and paraelectric phases. As a result of our calculations the band structure of the GeTe and SnTe have a direct gap (L-high symmetry point), which are 0.742 eV and 0.359 eV in the ferroelectric phase for GeTe and SnTe, respectively. In the paraelectric phase, the gaps are 0.376 eV and 0.028 eV for GeTe and SnTe, respectively. The valence band maximum results from the sp- hybridization of Ge and Te bands. The next lower

Table 1
The calculated equilibrium lattice parameters (a, and c) for GeTe and SnTe in ferroelectric and paraelectric phase

Material	Structure	Reference	*a* (Å)	*c* (Å)
GeTe	Rhombohedral (R3m)	Present	4.228	10.886
		Experimental[a]	4.156	10.663
	Cubic (Fm3m)	Present	6.024	
		Theory (GGA)[b]	6.011	
		Theory (LDA)[b]	5.858	
		Experimental[c]	5.996	
SnTe	Rhombohedral (R3m)	Present	4.502	11.489
	Cubic (Fm3m)	Present	6.309	
		Theory (GGA)[b]	6.404	
		Theory (LDA)[b]	6.231	
		Experimental[c]	6.327	

[a]Reference [7]; [b]Reference [22]; [c]Reference [23].

band to the valence band maximum merges with the valence band maximum on going from the L point along the high symmetry line to the Z point. On the whole, our calculations reproduce the essential features of the band structures of GeTe and SnTe, prominent among which is the arrangement of band symmetries at the L point in which the valence and conduction bands have L^+ and L^- symmetries and vice versa for SnTe and GeTe. The change in the energy gap for the SnTe and GeTe can be understood qualitatively in terms of the difference between the relativistic effect in Ge and Sn (spin-orbital coupling) and the relativistic correction is extremely important in determining the positions of the energy bands (such as a weak topological insulator). Furthermore our results are in agreement with the results obtained in previous calculations [7, 8]. We have summarized the band gap energies for SnTe and GeTe in Table 2 with previous theoretical and experimental results.

3.2. Optical Properties

It is well known that the effect of the electric field vector, $\mathbf{E}(\omega)$, of the incoming light is to polarize the material. At the level of a linear response, this polarization can be calculated using the following relation [28,29]:

$$P^i(\omega) = \chi^{(1)}_{ij}(-\omega, \omega).E^j(\omega), \tag{1}$$

where $\chi^{(1)}_{ij}$ is the linear optical susceptibility tensor and it is given by [30]

$$\chi^{(1)}_{ij}(-\omega,\ \omega) = \frac{e^2}{\hbar\Omega}\sum_{nm\vec{k}} f_{nm}(\ \vec{k}\ )\frac{r^i_{nm}(\vec{k})r^i_{mn}(\vec{k})}{\omega_{mn}(\vec{k})-\omega} = \frac{\varepsilon_{ij}(\omega)-\delta_{ij}}{4\pi} \tag{2}$$

Table 2
Energy band gap for GeTe and SnTe in ferroelectric and paraelectric phase

Material	Structure	Reference	$E_g(eV)$
GeTe	Rhombohedral (R3m)	Present	0.742 direct
	Cubic (Fm3m)	Theory[a]	0.48 direct
		Theory[b]	0.48
		Theory[c]	0.3369
		Present	0.376 direct
		Theory (LDA-GGA)[d]	0.399–0.340
		Experimental[d]	0.2
SnTe	Rhombohedral (R3m)	Present	0.359 direct
	Cubic (Fm3m)	Present	0.028 direct
		Theory (LDA-GGA)[d]	0.074–0.061
		Experimental[d]	0.2

[a]Reference [24]; [b]Reference [25]; [c]Reference [26]; [d]Reference [7, 27].

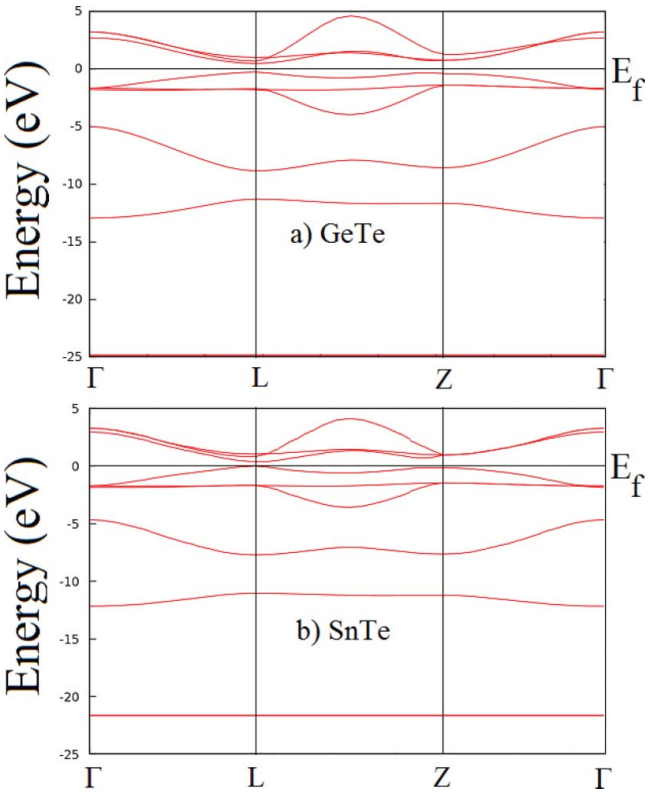

Figure 1. Energy band structure for GeTe and SnTe in ferroelectric phase.

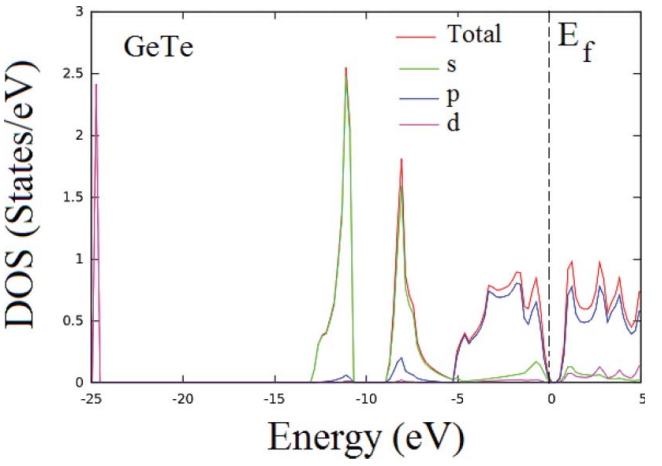

Figure 2. The total and projected density of states for GeTe in ferroelectric phase.

where n, m denote energy bands, $f_{mn}(\vec{k}) \equiv f_m(\vec{k}) - f_n(\vec{k})$ is the Fermi occupation factor, Ω is the normalization volume. $\omega_{mn}(\vec{k}) \equiv \omega_m(\vec{k}) - \omega(\vec{k})$ are the frequency differences, $\hbar\omega_n(\vec{k})$ is the energy of band n at wave vector **k.** The $\vec{r}_{nm}$ are the matrix elements of the position operator [30].

As can be seen in Eq. (2), the dielectric function $\varepsilon_{ij}(\omega) = 1 + 4\pi\chi_{ij}^{(1)}(-\omega,\ \omega)$ and the imaginary part of $\varepsilon_{ij}(\omega)$, $\varepsilon_2^{ij}(\omega)$, is given by

$$\varepsilon_2^{ij}(w) = \frac{e^2}{\hbar\pi}\sum_{nm}\int d\vec{k}\, f_{nm}(\vec{k})\frac{v_{nm}^i(\vec{k})v_{nm}^j(\vec{k})}{\omega_{mn}^2}\delta(\omega - \omega_{mn}(\vec{k})). \tag{3}$$

The real part of $\varepsilon_{ij}(\omega)$, $\varepsilon_1^{ij}(\omega)$, can be obtained by using the Kramers-Kroning transformation [30]. Because the Kohn-Sham equations determine the ground state properties, the unoccupied conduction bands as calculated, have no physical significance.

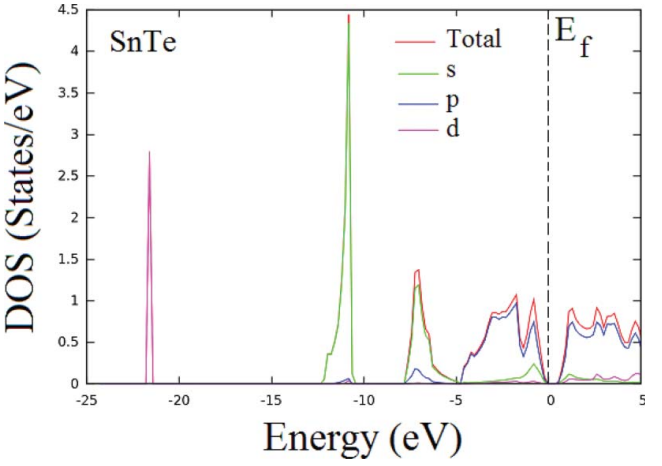

Figure 3. The total and projected density of states for SnTe in ferroelectric phase.

The known sum rules [31] can be used to determine some quantitative parameters, particularly the effective number of the valence electrons per unit cell N_{eff}, as well as the effective optical dielectric constant ε_{eff}, which make a contribution to the optical constants of a crystal at the energy E_0. One can obtain an estimate of the distribution of oscillator strengths for both intraband and interband transitions by computing the $N_{eff}(E_0)$ defined according to

$$N_{eff}(E) = \frac{2m\varepsilon_0}{\pi\hbar^2 e^2 Na} \int_0^\infty \varepsilon_2(E) E dE, \tag{4}$$

where N_a is the density of atoms in a crystal, e and m are the charge and mass of the electron, respectively, and $N_{eff}(E_0)$ is the effective number of electrons contributing to optical transitions below an energy of E_0.

Further information on the role of the core and semi-core bands may be obtained by computing the contribution that the various bands make to the static dielectric constant, ε_0. According to the Kramers-Kronig relations, one has

$$\varepsilon_0(E) - 1 = \frac{2}{\pi} \int_0^\infty \varepsilon_2(E) E^{-1} dE. \tag{5}$$

One can therefore define an 'effective' dielectric constant, that represents a different mean of the interband transitions from that represented by the sum rule, Eq. (5), according to the relation

$$\varepsilon_{eff}(E) - 1 = \frac{2}{\pi} \int_0^{E_0} \varepsilon_2(E) E^{-1} dE. \tag{6}$$

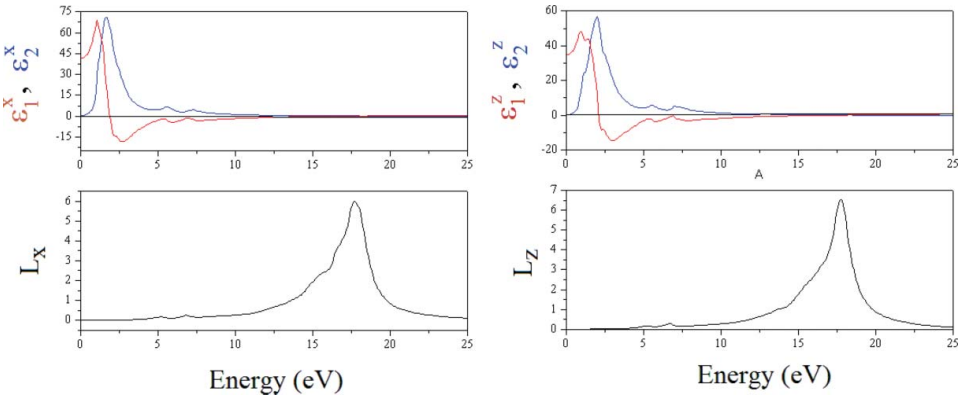

Figure 4. Energy spectra of dielectric function $\varepsilon = \varepsilon_1 - i\varepsilon_2$ and energy-loss function (L) along the x- and z-axes for GeTe in ferroelectric phase.

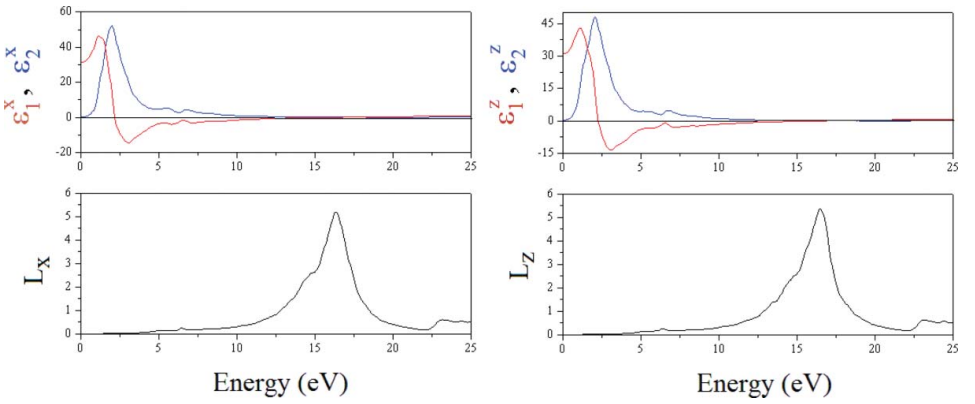

Figure 5. Energy spectra of dielectric function $\varepsilon = \varepsilon_1 - i\varepsilon_2$ and energy-loss function (L) along the x- and z-axes for SnTe in ferroelectric phase.

The physical meaning of ε_{eff} is quite clear: ε_{eff} is the effective optical dielectric constant governed by the interband transitions in the energy range from zero to E_0, i.e. by the polarization of the electron shells.

The GeTe and SnTe single crystals have a rhombohedral structure that is optically a uniaxial system. For this reason, the linear dielectric tensor of the GeTe and SnTe compounds has two independent components that are the diagonal elements of the linear dielectric tensor. We first calculated the real and imaginary parts of the linear dielectric function of the GeTe and SnTe compounds that have been along the x- and z-directions (Fig. 4 and Fig. 5). All the GeTe and SnTe compounds studied so far have $\varepsilon_1^x(\varepsilon_1^z)$ are equal to zero in the energy region between 1 eV and 18 eV for the decreasing $(d\varepsilon_1/dE < 0)$ and increasing $(d\varepsilon_1/dE > 0)$ of $\varepsilon_1(eV)$ (see Table 3). In addition, values of ε_1 versus photon energy have main peaks in the energy region between 0.3 eV and 5 eV. Some of the principal features and singularities of the ε_{ij} for both investigated compounds are shown in Table 3. The peaks of the ε_2^x and ε_2^z correspond to the optical transitions from the valence band to the conduction band and are in agreement with the previous results. The maximum peak values of ε_2^x and ε_2^z for GeTe are around 1.63 eV and 1.99 eV, respectively, whereas the maximum values of ε_2^x and ε_2^z for SnTe are around 1.99 eV and 2.05 eV, respectively. In general, there are various contributions to the dielectric function, but Fig. 4 and Fig. 5 show only the contribution of the electronic polarizability to the dielectric function. In the range between 0.5 eV and 4 eV, ε_1^z decrease with increasing

Table 3
Some of principal features and singularities of the linear optical responses for GeTe and SnSe in ferroelectric phase

Material	$\varepsilon_1(eV)$	$d\varepsilon_1/dE < 0$	$d\varepsilon_1/dE > 0$	$\varepsilon_2(eV)$	
GeTe	ε_1^x	1.19	17.45	$\varepsilon_{2,max}^x$	1.63
	ε_1^z	2.12	17.53	$\varepsilon_{2,max}^z$	1.99
GeTe	ε_1^x	2.23	16.07	$\varepsilon_{2,max}^x$	1.99
	ε_1^z	2.29	16.13	$\varepsilon_{2,max}^z$	2.05

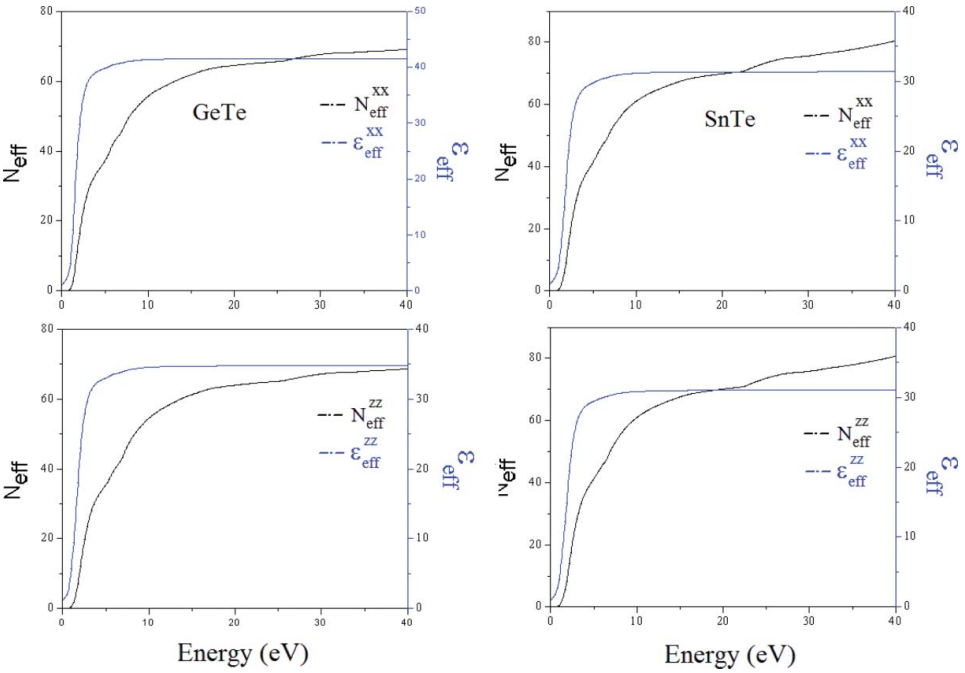

Figure 6. Energy spectra of N_{eff} and ε_{eff} along the x- and z- axes in ferroelectric phase.

photon-energy, which is characteristic of an anomalous dispersion. In this energy range, the transitions between occupied and unoccupied states mainly occur between s and p states that can be seen in the DOS and PDOS displayed in Fig. 2 and Fig. 3.

The corresponding energy-loss functions, $L(\omega)$, are also presented in Fig. 4 and Fig. 5. In this figure, L_x and L_z correspond to the energy-loss functions along the x- and z-directions. The function $L(\omega)$ describes the energy loss of fast electrons traversing the material. The sharp maxima in the energy-loss function are associated with the existence of plasma oscillations [32]. The curves of L_x and L_z in Fig. 4 and Fig. 5 have a maximum near 17.67 and 17.69 *eV* for GeTe, respectively and 16.32 and 16.50 *eV* for SnTe, respectively.

The calculated effective number of valence electrons N_{eff} and the effective dielectric constant ε_{eff} are given in Fig. 6. The effective number of valence electron per unit cell, N_{eff}, contributing in the interband transitions, reaches a saturation value at approx. 30 *eV*. This means that deep-lying valence orbitals participate in the interband transitions as well (see Fig. 1). The effective optical dielectric constant, ε_{eff}, shown in Fig. 6, reaches a saturation value at about 10 *eV*. This means that the greatest contribution to ε_{eff} arises from interband transitions between 0 and 10 *eV*.

Conclusion

In the present work, we have made a detailed investigation of the structural, electronic, and frequency-dependent linear optical properties of the GeTe and SnTe crystals using the density functional methods. The results of the structural optimization implemented using the GGA are in good agreement with the experimental and theoretical results. We have examined photon-energy dependent dielectric functions, some optical properties

such as the energy-loss function, the effective number of valance electrons and the effective optical dielectric constant along the x- and z-axes.

Funding

This work is supported by the projects DPT-HAMIT, DPT-FOTON, NATO-SET-193 and TUBITAK under Project Nos. 113E331, 109A015, 109E301. One of the authors (Ekmel Ozbay) also acknowledges partial support from the Turkish Academy of Sciences.

References

1. R. Shaltaf, E. Durgun, J.-Y. Raty, Ph. Ghosez, and X. Gonze, Dynamical, dielectric, and elastic properties of GeTe investigated with first-principles density functional theory. *Phys. Rev. B.* **78**, 205203 (2008).
2. M. Libera, and M. Chen, Time-resolved reflection and transmission studies of amorphous Ge-Te thin-film crystallization. *J. Appl. Phys.* **73**, 2272 (1993).
3. E. F. Steigmeier, and G. Harbeke, Soft Phonon Mode and Ferroelectricity in GeTe. *State Commun.* **8**, 1275–1279 (1979).
4. J. Y. Raty, V. V. Godlevsky, J. P. Gaspard, C. M. Bichara Bionducci, R. Bellissent, R. Céolin, J. R. Chelikowsky, and P. H. Ghosez, Local structure of liquid GeTe via neutron scattering and ab initio simulations. *Phys.Rev.B.* **65**, 115205 (2002).
5. N. E. Zein, V. I. Zinenko, and A. S. Fedorov, Ab Initio Calculations of Phonon Frequencies and Dielectrics Constants in A^4B^6 Compounds. *Phys. Lett. A.* **164**, 115–1196 (1992)
6. A. Onodera, I. Sakamoto, Y. Fujii, N. Mori, and Sugai, Structural and electrical properties of GeSe and GeTe at high pressure. *Phys. Rev. B.* **56**, 7935 (1997).
7. C. M. I. Okoye, Electronic and optical properties of SnTe and GeTe. *J.Phys.: Condens. Matter.* **14**, 8625 (2002).
8. Shin-Qing Shen, *Topological Insulators: Dirac Equation in Condensed Matter*. Berlin: Springer-Verlag; 2012.
9. Y. Tanaka, Z. Ren, T. Sato, K. Nakayama, S. Souma, T. Takahashi, Segawa, and K. Yoichi Ando, Experimental realization of a topological crystalline insulator in SnTe. *Nat. Phys.* **8**, 800–803 (2002).
10. T. H. Hsieh, H. Lin, J. Liu, W. Duan, A. Bansil, and L. Fu, Topological Crystalline Insulators in The Sntematerial Class. *Nat. Commun.* **3**, 982–988 (2012).
11. P. Dziawa, B. J. Kowalski, K. Dybko, R. Buczko, A. Szczerbakow, M. Szot, E. Łusakowska, T. Balasubramanian, B. M. Wojek, M. H. Berntsen, O. Tjernberg, and T. Story, Topological crystalline insulator states in $Pb_{1-x}Sn_xSe$. *Nature Mater.* **11**. 1023–1027 (2012).
12. S. Picozzi, Ferroelectrics Rashiba Semiconductors as a Novel Class of Multifunctional.
13. Z. M. Hasan, and J. E. Moore, Three-Dimensional Topological Insulators. *Matter Phys.* **2**, 55–78 (2011).
14. H. Koc, A. M. Mamedov, and E. Ozbay, Optical Properties and Electronic Band Structure of Topological Insulators(on $A_2^5B_3^6$ compound based). *Ferroelectrics*. **448**, 29–41 (2013)
15. G. Kresse, and J. Hafner, Ab initio molecular dynamics for liquid metals. *Phys Rev B.* **47**, 558–561.
16. G. Kresse, and J. Furthmüller, Ab-initio total energy calculations for metals and semiconductors using a plane-wave basis set. *Comput Mater Sci.* **6**, 15–50 (1996).
17. G. Kresse, and D. Joubert, From ultrasoft pseudopotentials to the projector augmented-wave method. *Phys Rev B.* **59**, 1758–1775 (1999).
18. G. Kresse, and J. Furthmüller, Efficient iterative schemes for ab initio total- energy calculations using a plane-wave basis set. *Phys Rev B.* **54**, 11169–11186 (1996)
19. P. Hohenberg, and W. Kohn, Inhomogeneous Electron Gas. *Phys. Rev.* **136**, A1133–A1138 (1964).

20. J. P. Perdew, and S. Burke, Ernzerhof M. Generalized gradient approximation made simple. *Phys Rev Lett.* **77**, 3865–3868 (1996).
21. H. J. Monkhorst, and J. D. Pack, Special points for Brillouin-zone intergrations. *Phys Rev B.* **13**, 5188–5192 (1976).
22. P. B. Pereira, I. Sergueev, S. Gorsse, J. Dadda, E. Müller, and R. P. Hermann, Lattice dynamics and structure of GeTe, SnTe and PbTe. *Phys. Status Solidi B.* **250**, 1300–1307 (2013).
23. T. Seddon, S. C. Gupta, and G. A. Saunders, Hole contribution to the elastic constants of SnTe. *Solid State Communications*. **20**, 69–72 (1976). B Hoston, and R. E. Strakna, *Bull. Am. Phys. Soc.* **9**, 646 (1964).
24. R. Shaltaf, E. J. Durgun, J. Y. Raty, P. H. Ghosez, and X. Gonze, Dynamical, dielectric, and elastic properties of GeTe investigated with first-principles density functional theory. *Phys. Rev. B.* **78**, 205203 (2008).
25. K. M. Rabe, and J. D. Joannopoulos, Theory of the structural phase transition of GeTe. *Phys. Rev. B.* **36**, 6631 (1987).
26. A. Ciucivara, B. R. Sahu, and L. Kleinman, Density functional study of the effect of pressure on the ferroelectric GeTe. *Phys. Rev. B.* **73**, 214105 (2006).
27. L. L. Chang, P. J. Stiles, and L. Esaki, *IBM J. Res. Rev.* **10**, 484 (1966).
L. Esaki, and P. J. Stiles, New Type of Negative Resistance in Barrier Tunneling. *Phys. Rev. Lett.* **16**, 1108 (1966).
28. Z. H. Levine, and D. C. Allan, Linear optical response in silicon and germanium including self-energy effects. *Phys Rev Lett.* **63**, 1719–1722 (1989).
29. Koc H, Deligöz E, and Mamedov AM: The elastic, electronic, and optical properties of PtSi and PtGe compounds. *Philosophical Magazine* 2011; **91**: 3093–3107.
30. H. R. Philipp, and H. Ehrenreich, Optical properties of semiconductors. *Phys Rev.* **129**, 1550–1560 (1963).
31. O. V. Kovalev, Representations of the crystallographic space groups. *Irreducible representations induced representations and corepresentations*. Amsterdam: Gordon and Breach; 1965.
32. L. Marton, Experiments on low-energy electron scattering and energy losess. *Rev Mod Phys.* **28**, 172–183 (1956).